Spring 5-2024

Evaluating the Accuracy of Different Remote Sensing Methods Used to Derive Absorption from Chromophoric Dissolved Organic Matter in Maine Estuaries

Andrea Rudai
University of Maine - Main, andreajeanr02@gmail.com

EVALUATING THE ACCURACY OF DIFFERENT REMOTE SENSING METHODS USED TO DERIVE ABSORPTION FROM CHROMOPHORIC DISSOLVED ORGANIC MATTER IN MAINE ESTUARIES

by

Andrea Rudai

A Thesis Submitted in Partial Fulfillment
of the Requirements for a Degree with Honors
(Marine Science)

The Honors College

University of Maine

May 2024

Advisory Committee:
Margaret Estapa, Assistant Professor of Oceanography, Advisor
Damian Brady, Agatha B. Darling Professor of Oceanography
James Brophy, Lecturer in Honors
Patrick Gray, Postdoctoral Research Assistant

ABSTRACT

Current knowledge of dissolved organic carbon (DOC) in Maine estuaries is based on limited field research. By using chromophoric dissolved organic matter (CDOM) as a proxy, it is possible to use satellite images to estimate the concentration of DOC in an entire body of water. This study aims to evaluate different methods that calculate absorption by CDOM from ocean color remote sensing using images taken by Landsat 9 of the Sheepscot, Penobscot, and Damariscotta rivers. The study revealed that although there were some similarities in along-estuary trends between the remotely-sensed absorption and absorption measured in situ, the algorithms that were evaluated did not adequately replicate the in situ results. There was also a consistent offset between the spectral slope derived from remote sensing and the spectral slope measured in situ. The spectral slope calculated from remote sensing was consistently higher than the spectral slope measured in situ, which could indicate that the absorption values calculated from current remote sensing methods will be less accurate at shorter wavelengths. An explanation for the lack of accuracy in the remote sensing methods evaluated is that the assumptions made by the methods are not applicable to the Sheepscot, Penobscot, or Damariscotta rivers. Although this study does not have enough data to make any definitive statements on the effectiveness of current methods to derive absorption from remote sensing, it is clear that future research on this topic should focus on matching spectral slopes to those measured in situ.

ACKNOWLEDGEMENTS

I would like to thank my advisor, Dr. Margaret Estapa for all of her guidance and help with this project. I truly would not be able to create this thesis without her help. I would like to thank Camille Michaud for allowing me to use her data to evaluate different remote sensing methods. I would like to thank my committee, Dr. Damian Brady. Dr. James Brophy, and Dr. Patrick Gray, for their guidance and expertise. I would also like to thank NASA for funding this project. Finally, I would like to thank my friends and family for their love and support.

TABLE OF CONTENTS

LIST OF FIGURES

INTRODUCTION

Dissolved organic carbon (DOC) refers to any piece of carbon that originates from a living organism and is smaller than one micron. Dissolved organic carbon comprises 80-90% of the coastal ocean's total organic carbon (Cao et al. 2018). Dissolved organic carbon in estuarine and coastal systems can provide a critical link between the terrestrial and aquatic carbon cycles (Cao et al. 2018). There has recently been more research that attempts to understand DOC as a dynamic component of the carbon cycle (Fichot et al. 2023). The previous understanding of DOC was limited to in situ measurements, which only provide small points of reference for DOC in the marine environment (Cao and Tzortziou, 2021). Being able to use remote sensing to measure DOC would allow for the DOC concentrations of an entire body of water to be mapped out.

To measure DOC from remote sensing, it is necessary to use absorption from chromophoric dissolved organic matter (CDOM) (Werdell et al. 2018). Chromophoric dissolved organic matter is dissolved organic matter that absorbs light, namely blue and ultraviolet light (Fichot et al. 2023). A major source of CDOM is terrestrial plants (Mannino et al. 2014). There is a strong correlation between CDOM and DOC in coastal environments (although there is seasonal variation) so absorption from CDOM is used as a proxy to calculate DOC. Because of this, being able to accurately remotely-sense absorption from CDOM (a_{CDOM}), especially at lower wavelengths, is key to being able to accurately remotely-sense DOC (Fichot et al. 2023).

Absorption is an inherent optical property (IOP) which is a property of water that does not depend on changes in the amount of light (Werdell et al. 2018). Inherent optical properties like a_{CDOM} cannot be directly measured by remote sensing but they can be estimated from apparent optical properties (AOP) which are properties of water that do depend on the amount of light (Werdell et al. 2018). Satellites measure the radiance of the top of the atmosphere. This can be used to calculate the AOP remote sensing reflectance (R_{rs}), which refers to the fraction of incoming light that is reflected off the water in the hypothetical scenario where there is no atmosphere, and the sun is at its zenith (Werdell et al. 2018). Many different methods have been developed to calculate absorption from R_{rs} (Werdell et al. 2018).

Most traditional ocean color satellites like MODIS and MERIS have low spatial resolution and cannot be used to remotely sense estuaries. The satellites Landsat 8 and 9 have high spatial resolution, which are able to capture images of the estuaries which are the focus of this study. Landsat 8 and 9 are meant to study images of land but they have been proven adequate for studying marine environments (Pahlevan et al. 2016). Landsat has been used to find a_{CDOM} in other inland waters (Alcântara et al. 2016) but it has not been used to find absorption in estuaries that feed into the Gulf of Maine. Using remote sensing to measure the absorption of estuaries can be complicated because of how optically complex estuaries are compared to the coastal ocean (Fichot et al. 2023).

It is important to learn the best way to accurately measure absorption in estuaries as it is a critical step in being able to measure DOC from remote sensing. Being able to evaluate the DOC content of an entire estuary could help to broaden understanding of the link between the terrestrial and marine carbon cycles. The first step in accomplishing that goal is to evaluate the effectiveness of current remote sensing methods to calculate absorption in estuarine environments. This study aims to evaluate the efficacy of current remote sensing methods for calculating absorption of the Sheepscot, Penobscot, and Damariscotta river estuaries.

METHODS

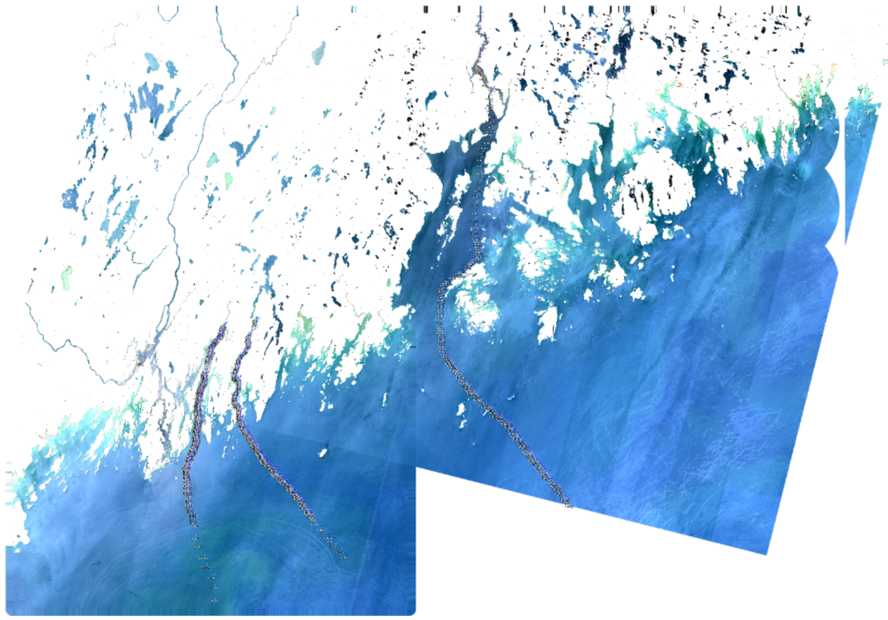

Fig. 1 shows a quasi-true color Landsat 9 Operational Land Imager (OLI) image of the study area. Taken August 3rd, 2023.

Study Area

Figure 1 shows the area of study. The rivers of interest are the Sheepscot, Penobscot, and Damariscotta. The Penobscot has a large watershed of 8,570 square miles (Maine Rivers, 2024) and drains from half of the state while the Damariscotta and Sheepscot are small and have watersheds of 103 and 320 square miles respectively (Maine Rivers, 2024, Rudoff et al. 1995). The Damariscotta is a well-mixed estuary, the Sheepscot is partially mixed, and the Penobscot has varied mixing throughout (Mayer et al. 1996, Haefner, 2011). The Damariscotta has more chlorophyll than the Sheepscot River (Mayer et al. 1996).

To examine changes in the water properties along each estuary, points were chosen in a line down the center of the river. The starting points were chosen by observing the northernmost point in the river that was visible. The northernmost point in these rivers is the head, which has the least marine influence. The end of the transects reaches out into the Gulf of Maine (GoM) as remote sensing in the coastal ocean is regarded as having fewer challenges than in estuaries and inland waters (Fichot et al. 2024).

Satellite

This study was conducted using products from Landsat 9's Operational Land Imager (OLI) which has four visible spectral bands at the wavelengths 443, 482, 561, and 655 nm. The image used in this study was captured on August 3rd, 2023. This date was chosen because it had less than 10% cloud cover, which is optimal for remote sensing. It was also selected because it was in the same season as in situ samples that were collected in a companion study (Michaud, 2024). The algorithms used required level 1b data, which was taken from USGS EarthExplorer (USGS, 2024). The image was atmospherically corrected following the same process as was used by Snyder et al. (2017). The atmospheric correction and multiple absorption algorithms were applied in NASA's SeaDAS software (NASA, 2024). The products were further analyzed on Sentinel Application Platform (SNAP) which is a free program used specifically for visualizing and analyzing remote sensing data.

Equations

There were three different algorithms used to calculate absorption from R_{rs}. Two of these, Loisel et al. 2018 (LS2) and Lee et al. 2002 (QAA), are semi-analytical algorithms that are based on models of light in water. These absorption algorithms give total absorption, which is dominated by CDOM in Maine estuaries. The algorithm from Mannino et al. 2014 (MLRa) is empirical and fits a line to existing CDOM absorption and R_{rs} data to relate CDOM absorption at 443 nm ($a_{CDOM}(443)$) and R_{rs}. The LS2 algorithm calculates the absorption by relating the diffuse attenuation coefficient ($K_d(\lambda)$) and R_{rs} (Loisel et al. 2018). The LS2 algorithm determines the $K_d(\lambda)$ value using satellite data which requires an assumption about the chlorophyll concentration in the water. The LS2 algorithm does not make any assumptions about the ratios of R_{rs} at different wavelength. The QAA algorithm uses assumptions about the ratios between R_{rs} bands to evaluate the absorption (Lee et al. 2002 and 2007). The QAA algorithm was developed from data collected in offshore waters. The MLRa equation was developed for SeaWiFS and MODIS by fitting R_{rs} from MODIS and SeaWiFS to a curve using in situ data taken on days where the satellites would be overhead from the northeastern U.S. waters from 2004 to 2011 (Mannino et al. 2014).

Two remote sensing absorptions were generated using the LS2 and QAA algorithms' default configurations in SeaDAS l2gen software (Loisel et al. 2018, Lee et al. 2002 and 2004). The MLRa absorption was calculated later in Matlab (Mannino et al. 2014). Below is the MLRa equation implemented at Landsat wavelengths in this study to determine the absorption at 443 nm (Equation 1). The original equation was developed for SeaWiFS and required $R_{rs}(443)$ and $R_{rs}(555)$ as input. This study used $R_{rs}(443)$ and $R_{rs}(561)$ from Landsat 9 OLI as inputs.

(1) $$ln\left(a_{CDOM}(443)\right) = -3.379 - 1.1513 \cdot ln\left(R_{rs}(443)\right) + 1.006 \cdot ln\left(R_{rs}(561)\right)$$

Mannino et al. (2014) also developed an equation that could be used to determine the spectral slope from 300 to 600 nm ($S_{300\text{-}600}$) from R_{rs} (Equation 2). The spectral slope is the exponential decay coefficient of absorption from CDOM as a function of wavelength. This can be seen in equation 2, which inputs wavelength and outputs absorption from CDOM at that wavelength. In this equation, $a_{CDOM}(\lambda)$ represents absorption from CDOM at wavelength λ nm, $a_{CDOM}(\lambda_o)$ represents absorption from CDOM at reference wavelength λ_o nm, and S_{CDOM} represents the spectral slope of CDOM. Ideally spectral slope is specified over an explicit wavelength range (Twardowski et al. 2004).

(2) $$a_{CDOM}(\lambda) = a_{CDOM}(\lambda_\circ) \cdot e^{-S_{CDOM}(\lambda-\lambda_\circ)}$$

This equation (MLRs) was developed in the same fashion as MLRa and will be used in the same fashion as MLRa in this study.

(3) $$\ln(S_{300-600}) = -3.679 + 0.168 \cdot \ln\left(R_{rs}(443)\right) - 0.134 \cdot \ln\left(R_{rs}(561)\right)$$

Reference Data

The in situ data that were used to evaluate the viability of these different algorithms was taken from Michaud (2024). The Penobscot River was sampled from a vessel on June 26, 2023. The Damariscotta River was sampled by wading into the river on August 1st, 2023. The Sheepscot River was sampled the same as the Damariscotta on August 16th, 2023. The CDOM spectral absorption by filtered samples from each estuary was measured using a benchtop spectrophotometer as described by Michaud (2024).

RESULTS

As shown in Figure 2, remote sensing reflectance at 655 nm ($R_{rs}(655)$) is 0.006 sr^{-1} at the head and mouth of the Sheepscot River but is 0.003 sr^{-1} where the river feeds into the Gulf of Maine (GoM). Remote sensing reflectance at 561 nm ($R_{rs}(561)$) is 0.011 sr^{-1} at the head and mouth of the river and 0.007 sr^{-1} where the Sheepscot River feeds into the GoM. Remote sensing reflectance at 443 nm ($R_{rs}(443)$) and remote sensing reflectance at 482 nm ($R_{rs}(482)$) are very similar, with both being measured to be 0.008 sr^{-1} at the head of the river, 0.010 sr^{-1} at the mouth of the river and approaching 0.006 sr^{-1} where the Sheepscot feeds into the GoM. For most of the transect, $R_{rs}(482)$ is greater than $R_{rs}(443)$.

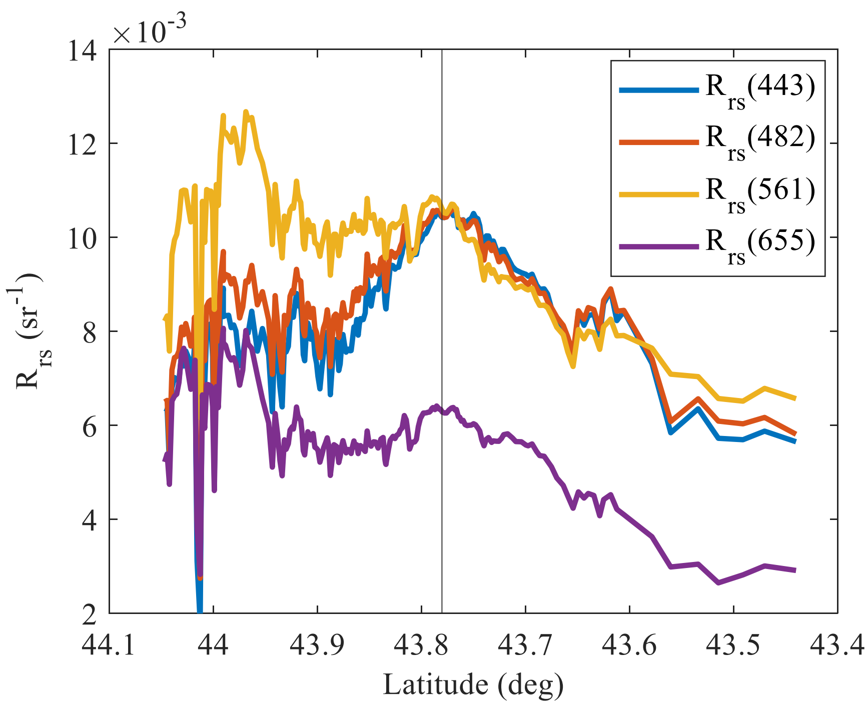

Fig. 2 shows the remote sensing reflectance (R_{rs}) of the Sheepscot River with respect to latitude. The R_{rs} in the graphs are the wavelengths 443 (blue), 482 (red), 561 (yellow), and 655 nm (violet). The point with the greatest latitude is the head of the river and the gray line indicates the mouth of the river where the river feeds into the Gulf of Maine. The data was collected from images taken by Landsat 9 OLI on August 3rd, 2023.

Overall, the Penobscot River has both the lowest reflectance and the lowest amount of variation between each of the R_{rs} values as shown in Figure 3. $R_{rs}(655)$ measures 0.006 sr^{-1} at the head of the river, but then goes to 0.0035 sr^{-1} at the mouth of the river and where the river feeds into the GoM. At the head of the river, the values of $R_{rs}(561)$ are 0.0065 sr^{-1}, at the mouth of the river, the values approach 0.007 sr^{-1} and where the river feeds into the GoM, the values approach 0.0075 sr^{-1}. The values of $R_{rs}(443)$ and $R_{rs}(482)$ are similar to $R_{rs}(655)$ at the head of the river but become more like $R_{rs}(561)$ at the mouth of the river. Throughout the transect, $R_{rs}(482)$ is greater than $R_{rs}(443)$.

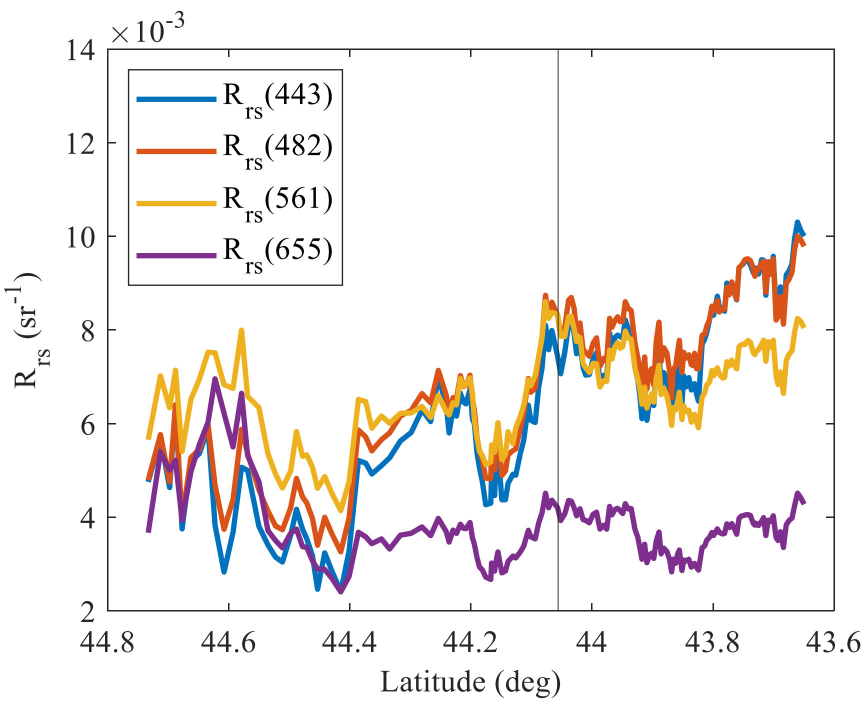

Fig. 3 shows the remote sensing reflectance (R_{rs}) of the Penobscot River with respect to latitude. The R_{rs} in the graphs are the same as in Figure 2. The data was collected from images taken by Landsat 9 OLI on August 3rd, 2023.

In general, the Damariscotta River has the highest R_{rs} values among the rivers being studied as shown in Figure 4. At the head of the Damariscotta, the values of $R_{rs}(655)$ are measured to be 0.0065 sr^{-1}. At the mouth of the river, the values of $R_{rs}(655)$

approach 0.005 sr^{-1}. Where the river feeds into the GoM, the values of R_{rs} are 0.003 sr^{-1}. $R_{rs}(561)$ is 0.0135 sr^{-1} at the head of the river, 0.009 sr^{-1} at the mouth of the river, and 0.007 sr^{-1} where the river feeds into the GoM. The values of $R_{rs}(443)$ and $R_{rs}(482)$ are similar for the entire length of the plot measured. At the head of the river, the values of $R_{rs}(443)$ and $R_{rs}(482)$ are around the same as the values of $R_{rs}(655)$. At the mouth and outflow of the Damariscotta, $R_{rs}(443)$ and $R_{rs}(482)$ become similar to $R_{rs}(561)$. Overall, $R_{rs}(482)$ is slightly greater than $R_{rs}(443)$.

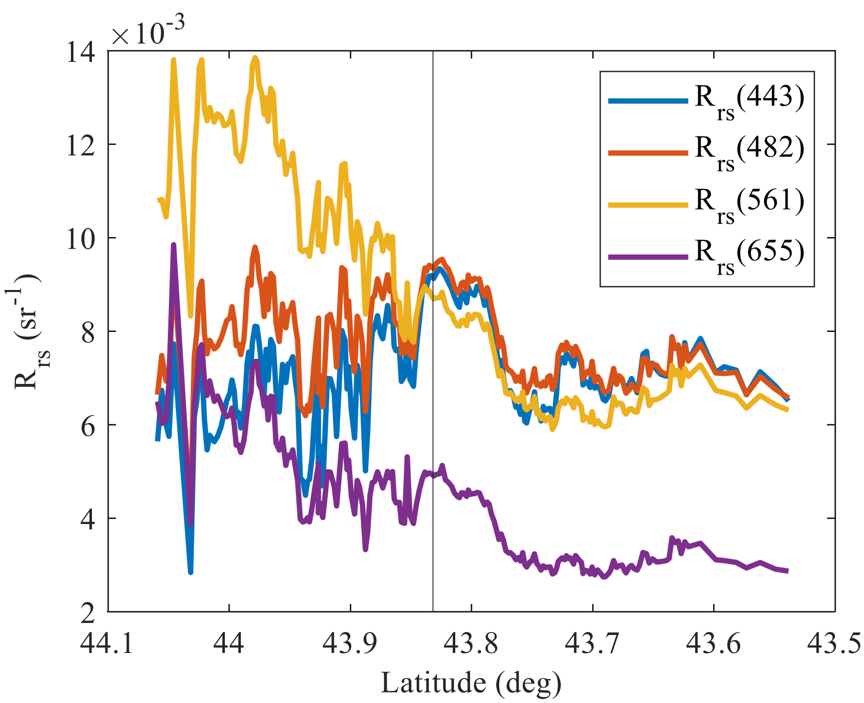

Fig. 4 shows the remote sensing reflectance (R_{rs}) of the Damariscotta River with respect to latitude. The R_{rs} in the graphs are the same as in Figure 2. The data was collected from images taken by Landsat 9 OLI on August 3rd, 2023.

In general, $R_{rs}(561)$ is the highest of all the wavelengths in each river before it reaches the Gulf of Maine (GoM). $R_{rs}(655)$ starts around the same as $R_{rs}(443)$ and $R_{rs}(482)$ but approaches 0.003 sr^{-1} as it reaches the coast of the GoM. At the head of each river, $R_{rs}(443)$ and $R_{rs}(482)$ are lower than $R_{rs}(561)$ but at the mouth of the river, $R_{rs}(443)$

and $R_{rs}(482)$ reach the same values as $R_{rs}(561)$ and become greater than $R_{rs}(561)$ in the GoM.

Looking at Figures 5, 6, and 7, the absorption calculated from remote sensing was less than the absorption measured in situ. The in situ measurements were located in different locations than the remote sensing transects, with many of the in situ measurement locations being closer to shore (Michaud, 2024). Overall, QAA yielded the highest absorption for each river out of the three methods used. The absorptions calculated using equations developed by Mannino et al. 2014 (MLRa) were consistently the lowest. The method developed by Loisel et al. (2018) (LS2) was in between QAA and MLRa but was closer to the MLRa values. The QAA values have a larger change with respect to latitude than the LS2 and MLRa absorption values. Each method's values level out where the rivers feed into the GoM.

The Sheepscot River's absorption values calculated from remote sensing are, in general, less than the values measured in situ (as seen in Figure 5a and 5b). The QAA absorption is 0.7 m^{-1} at the head of the river, 0.45 m^{-1} at the mouth of the river, and 0.35 m^{-1} where the Sheepscot feeds into the GoM. The LS2 absorption is 0.2 m^{-1} at the head of the river, 0.08 m^{-1} at the mouth of the river, and 0.075 m^{-1} where the Sheepscot feeds into the GoM. The MLRa absorption is 0.1 m^{-1} at the head of the river, 0.068 m^{-1} at the mouth of the river, and 0.065 m^{-1} where the Sheepscot feeds into the GoM. The first three in situ absorption measurements range from 5.96 to 2.88 m^{-1} (Michaud, 2024) and are greater than any of the values measured by remote sensing by at least 2 m^{-1}. The last three in situ absorption measurements range from 0.87 to 0.45 m^{-1} (Michaud, 2024) which is closer to the range of the remotely-sensed absorption values.

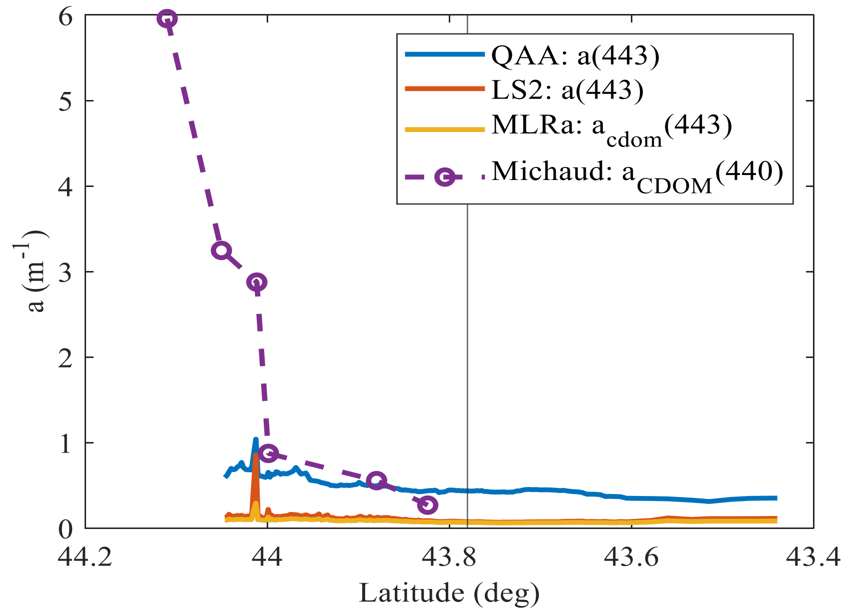

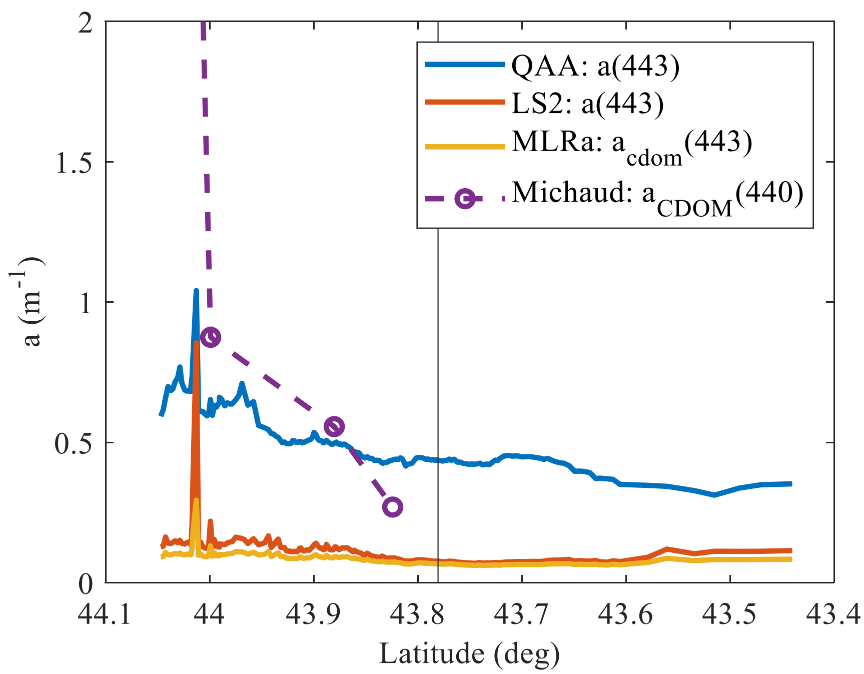

Fig. 5a and 5b show the absorption of water at 443 nm with respect to latitude in the Sheepscot River. Both figures show the same data, just at different scales. The measured and modeled absorption values represented in the graph are from remote sensing algorithms: QAA (blue), LS2 (red), and MLR (yellow), and measured in situ: Michaud (2024) (violet). The point with the greatest latitude is the head of the river and the gray line indicates the mouth of the river where the river feeds into the Gulf of Maine.

The Penobscot River's remote sensing absorption (as seen in Figure 6a and 6b) is consistently at least 1.19 m^{-1} less than the in situ absorption. The QAA absorption is 1.2

m^{-1} at the head of the river, 0.39 m^{-1} at the mouth of the river, and 0.32 m^{-1} where the Penobscot feeds into the GoM. The LS2 absorption is 0.15 m^{-1} at the head of the river, 0.09 m^{-1} at the mouth of the river, and 0.05 m^{-1} where the Penobscot feeds into the GoM. The MLRa absorption is 0.09 m^{-1} at the head of the river, 0.075 m^{-1} at the mouth of the river, and 0.053 m^{-1} where the Penobscot feeds into the GoM. The absorption measured in situ ranges between 3.77 m^{-1} and 2.67 m^{-1} (Michaud, 2024). Although the values differ, both the in situ absorption and remote sensing absorption show an increase and then decrease from north to south in the stretch of the river.

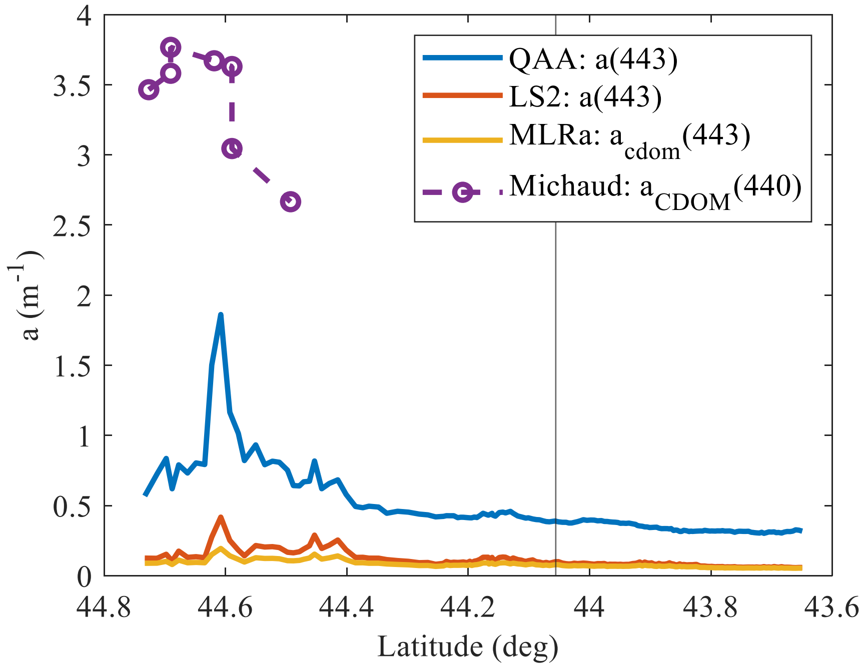

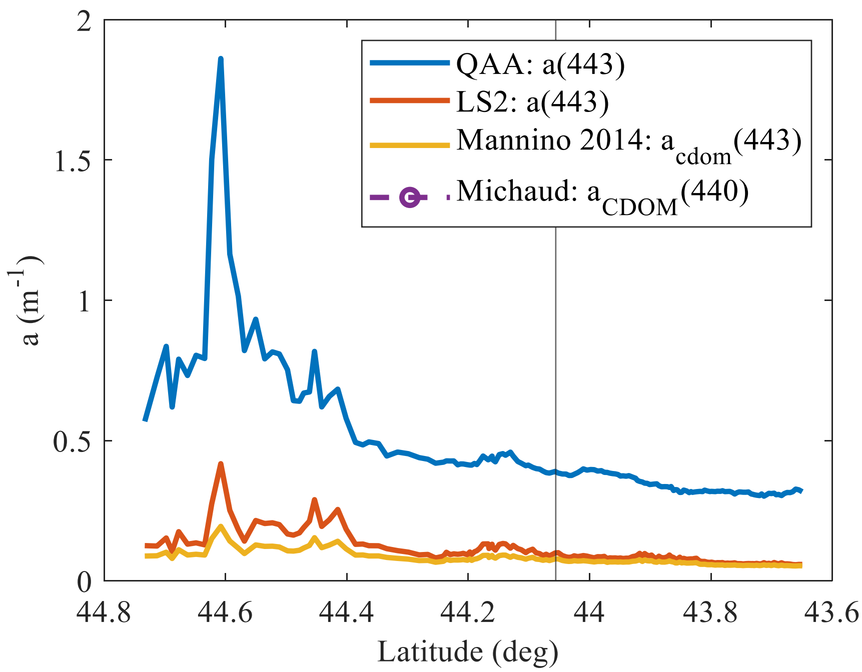

Fig. 6a and 6b show the absorption of water at 443 nm with respect to latitude in the Penobscot River. The absorptions represented in the graph are the same as in Figures 5a and 5b.

The Damariscotta River has the lowest absorption values overall (as seen in Figure 7a and 7b). The QAA absorption is 0.84 m^{-1} at the head of the river, 0.39 m^{-1} at the mouth of the river, and 0.31 m^{-1} where the Damariscotta feeds into the GoM. Ignoring any spikes, the LS2 absorption is 0.32 m^{-1} at the head of the river, 0.10 m^{-1} at the mouth of the river, and 0.08 m^{-1} where the Damariscotta feeds into the GoM. The MLRa absorption is 0.23 m^{-1} at the head of the river, 0.067 m^{-1} at the mouth of the river, and 0.065 m^{-1} where the Damariscotta feeds into the GoM. The Damariscotta River's remote sensing absorption values are closer to the in situ values than the other rivers discussed. The in situ absorption measurements range from 1.49 to 0.20 m^{-1}, which is close to the range of the absorption derived from remote sensing which is 0.84 to 0.065 m^{-1}. The sixth in situ measurement was taken from an enclosed area dominated by seaweed (Michaud, 2024) and does not follow the trend the rest of the in situ measurements follow.

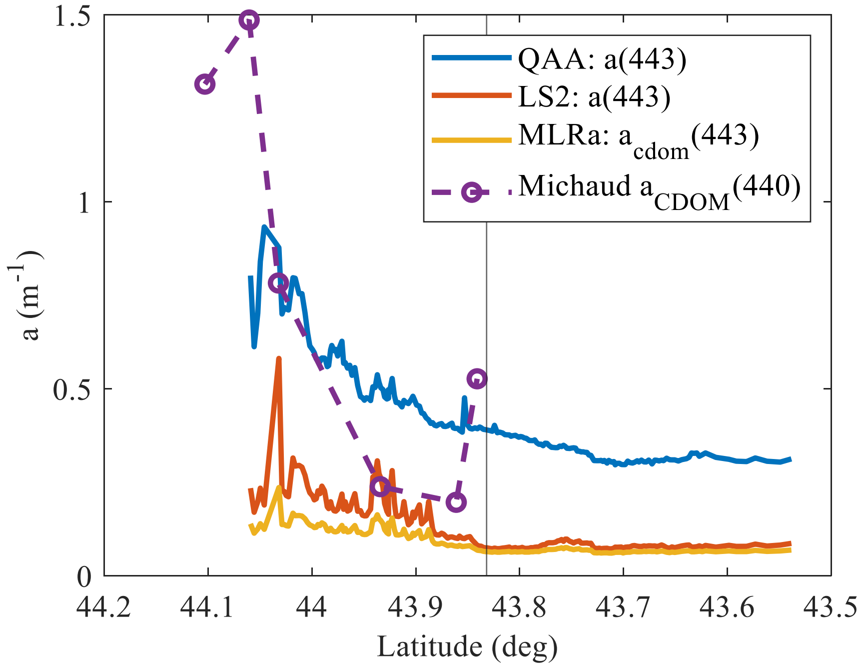

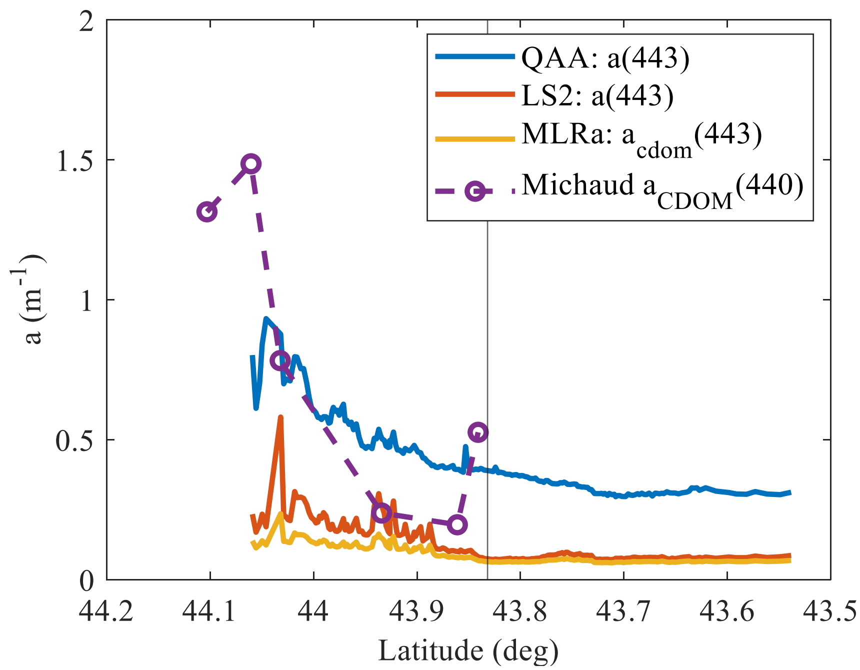

Fig. 7a and 7b shows the absorption of water at 443 nm with respect to latitude of the Damariscotta River. The absorptions represented in the graph are the same as in Figures 5a and 5b.

The absorptions measured with remote sensing are similar in value, regardless of which river with the Sheepscot absorption ranging from 0.05-1.00 m^{-1}, the Penobscot absorption ranging from 0.05-1.7 m^{-1}, and the Damariscotta absorption ranging from 0.06-0.9 m^{-1}. This is different from the in situ measurements; with the Sheepscot absorption ranging from 0.27-5.96 m^{-1}, the Penobscot absorption ranging from 2.67-3.77 m^{-1}, and the Damariscotta absorption ranging from 0.20-1.49 m^{-1}.

Looking at Figures 8, 9, and 10, the spectral slopes calculated from remote sensing using Equation 2 are greater than the spectral slopes measured in situ data. Despite the offset, the spectral slope values follow the same trends in terms of change in spectral slope with respect to latitude. Each estuary had an individual consistent offset between remote sensing and in situ spectral slope. Ignoring any spikes, the Sheepscot River's MLRs spectral slope values (as seen in Figure 8) range from 0.019-0.022 nm^{-1} and the in situ spectral slope values range from 0.0146-0.0178 nm^{-1}. The highest offset for the Sheepscot is 0.0054 nm^{-1}, the lowest offset is 0.0035 nm^{-1}, and the average offset is 0.0047 nm^{-1}. The Penobscot River's MLRs spectral slopes range from 0.0213-0.0192 nm^{-1} and the in situ spectral slopes range from 0.0146-0.0151 nm^{-1}. The offsets range from 0.0023-0.0058 nm^{-1} with the average offset being 0.0052 nm^{-1}. The MLRs' spectral slopes from the Damariscotta River (as seen in Figure 10) range from 0.019-0.022 nm^{-1} and the in situ spectral slopes, ignoring the last point, range from 0.0159-0.0184 nm^{-1}. The offset between the MLRs and in situ spectral slopes ranges from 0.0023-0.0034 nm^{-1}, with the average being 0.0027 nm^{-1}.

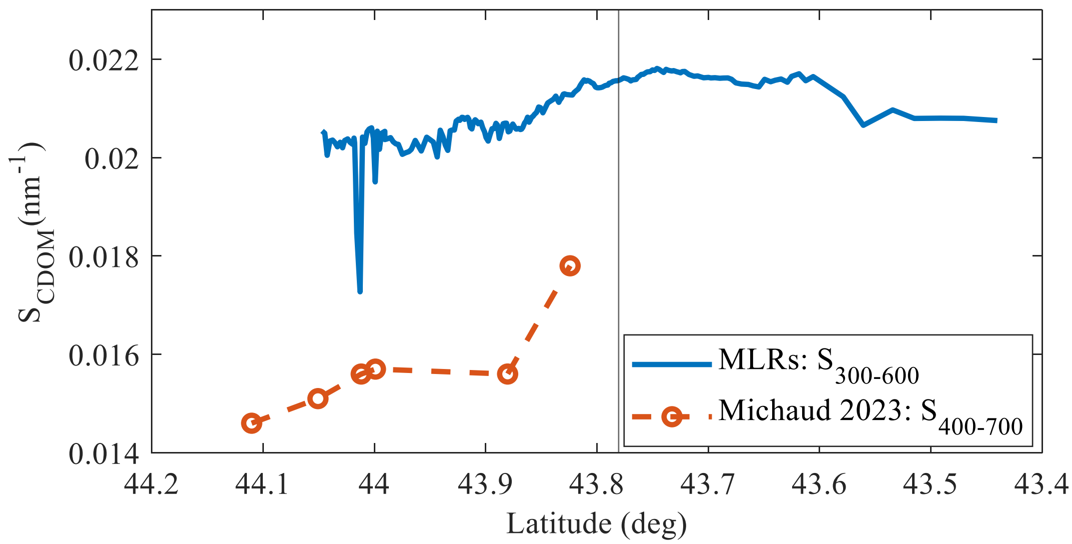

Fig. 8 shows the spectral slopes of the Sheepscot River with respect to latitude. The spectral slopes represented are $S_{300\text{-}600}$ from Mannino's equations (blue) and $S_{400\text{-}750}$ from Michaud (orange). The point with the greatest latitude is the head of the river and the gray line indicates the mouth of the river where the river feeds into the Gulf of Maine.

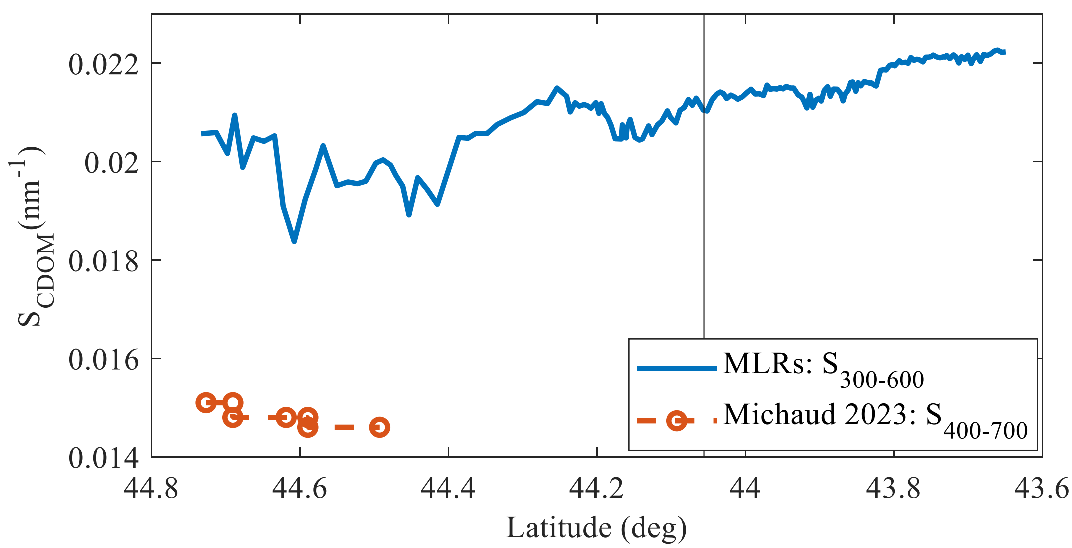

Fig. 9 shows the spectral slopes of the Penobscot River with respect to latitude. The spectral slopes are represented the same as in Figure 8.

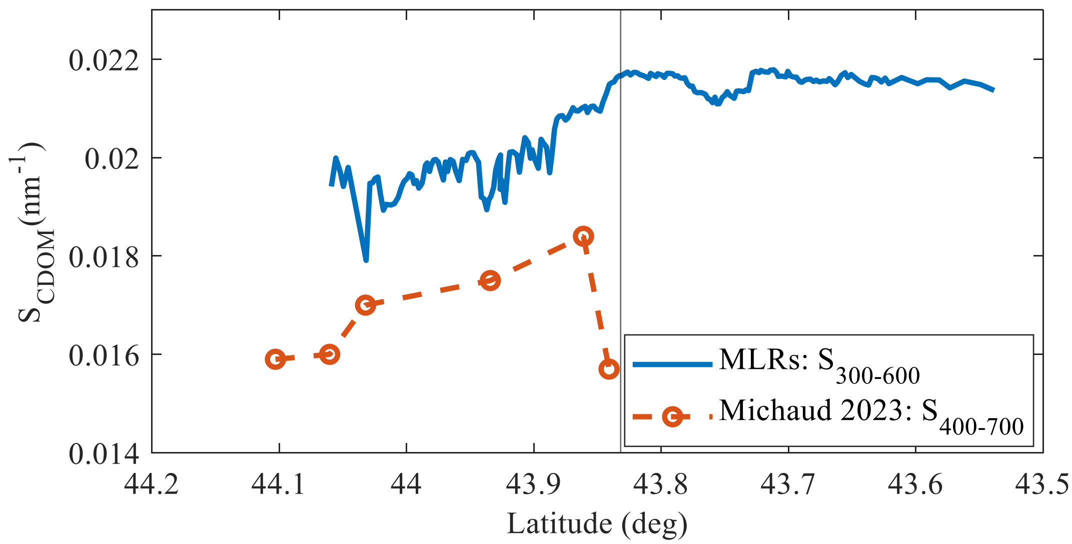

Fig. 10 shows the spectral slopes of the Damariscotta River with respect to latitude. The spectral slopes are represented the same as in Figure 8.

DISCUSSION

As seen in Figures 2, 3, and 4, the estuaries in this study differ in terms of the amount of each wavelength they reflect. One would expect there to be the same amount of variation in the absorption derived using these reflectances. However, this is not shown in the absorption derived from remote sensing in Figures 5, 6, and 7.

Out of the three rivers being studied, the Damariscotta River returned the most accurate results as both its absorption and spectral slope derived from remote sensing were the closest to the in situ values. In the Sheepscot River, the values of absorption at 443 nm (a(443)) from remote sensing were closer to the in situ values at the mouth and less close to the in situ values at the head. In the Penobscot River, the absorption and spectral slopes derived from remote sensing were the farthest off the in situ values. In addition to the marginal accuracy in absorption, the spectral slopes derived from remote sensing were greater than the in situ values. Although there are some a(443) values derived from remote sensing that are similar to the in situ values of a(440), this study indicates that the current remote sensing methods of calculating absorption are inaccurate when applied to estuaries on the Gulf of Maine. This study has helped to indicate where future research in developing methods to derive absorption by CDOM from remote sensing in the Gulf of Maine should focus.

There are a few possible reasons for errors that were independent of the remote sensing models used in this study. One possible reason could be that the atmospheric correction used could be a source of error. Another explanation is the difference in absorption could be due to differences in the exact placements of the in situ and remote sensing transects. The in situ measurements taken in the Damariscotta and Sheepscot rivers were sampled closer to the shore (Michaud, 2024) whereas the transect selected to collect the remote sensing data was in the middle of the river. This could have contributed to differences in absorption from CDOM as runoff from land and marshes is a major contributor of CDOM (Coble, 2007). The in situ measurements for the Penobscot River were taken from a vessel, but there was heavy rain on sampling day (Michaud, 2024). Rain causes there to be more runoff which could have caused an increase in CDOM in the river (Balch et al. 2016). Another possible reason for differences from remote sensing estimates is the difference in the date the data was collected. It is recommended that in situ measurements should be taken within 24 hours of the satellite passing overhead because of how much water can change, particularly due to tides (Cao et al. 2018). The Damariscotta River was the closest to having a match up in time and space as the in situ data were taken August 1st, 2023 (Michaud, 2024) and the date the Landsat image used in this study was captured was August 3rd, 2023.

Regardless of any error caused by environmental factors, the absorption derived from remote sensing should still resemble the absorption measured in situ. The amount of discrepancy in the remotely sensed absorption data is not adequately explained by these factors.

One explanation for the inaccuracies in remotely-sensed absorption and spectral slope could be that the assumptions made by the remote sensing models do not fit the estuaries chosen in the study. The LS2 model assumes information on the concentration of chlorophyll to derive $K_d(\lambda)$ (Loisel et al. 2018). The amount of chlorophyll and K_d are especially difficult to estimate at the head of the river where there is the most freshwater influence, especially for the Sheepscot, which has low chlorophyll content throughout

(Mayer et al. 1996). The QAA algorithm is sensitive to error from atmospheric correction (Werdell et al. 2018). The QAA algorithm makes assumptions about how the spectral slope of backscattering depends on the reflectance ratios between green and blue wavelengths and was developed for offshore waters (Lee et al. 2002 and 2007). The reflectance ratios of the coastal and open ocean differ from the ones found in Maine estuaries because further offshore, the total absorption is governed by phytoplankton at blue and green wavelengths (Fichot et al. 2023). In estuaries, there is a variable amount of CDOM that absorbs blue and green light and there are particles that scatter light at red wavelengths (Fichot et al. 2023). This phenomenon is shown in Figures 2, 3, and 4, as $R_{rs}(655)$ is greater at the head of the estuary compared to where the estuary feeds into the Gulf of Maine. The MLRa and MLRs empirical methods were made by fitting R_{rs} and matching absorption by CDOM data that was collected from the east coast to a multiple linear regression curve (Mannino et al. 2014). It was developed for the coastal ocean where phytoplankton have more influence on total absorption. The Damariscotta has a high concentration of chlorophyll and has a higher ocean contribution than the other rivers (Mayer et al. 1996) which could be the reason why the a(443) derived from remote sensing matches the most with the in situ measurements in the Damariscotta river and the mouth of the Sheepscot river, where there is more influence from marine water (Michaud, 2024). Conversely, the Sheepscot and Penobscot rivers have more freshwater influence (Michaud, 2024). This could explain why the absorption values derived from remote sensing are farther from the values measured in situ for the head of the Sheepscot River and the Penobscot River.

The range along the full estuary transect of the a(443) values derived from remote sensing using the MLRa method in each river were much closer to each other in magnitude and lower than the range of a(440) values measured in situ for each river. A possible reason for inaccuracies could be the result of the spectral slope derived from remote sensing being greater than the spectral slope measured in situ by approximately 0.0052, 0.0027, and 0.0047 nm^{-1} (respectively for the Penobscot, Damariscotta, and Sheepscot). The spectral slope from 300 to 600 nm ($S_{300-600}$) calculated using Equation 3 was consistently greater than the spectral slope from 400 to 750 nm ($S_{400-750}$) that was measured in situ. Even though the spectral slopes cover different wavelength ranges, mathematically there should not be such large differences in spectral slopes as spectral slope is the exponential decay coefficient of absorption which would not be expected to change much or at all with respect to changes in wavelength. In Equation 2, a_{CDOM} increases as wavelength decreases. Even if the absorption is accurate at longer wavelengths, an incorrect spectral slope assumption will cause absorption to vary for shorter wavelengths and the discrepancies will become more obvious as the greater the spectral slope, the slower absorption will increase as wavelength decreases. Therefore, an incorrect spectral slope assumption is not ideal if the goal is to find CDOM as it has a higher absorption at shorter wavelengths.

The difference in the spectral slope could be the reason that the absorption from remote sensing does seem to follow similar trends to the in situ absorption while also having a smaller range. For example, in Figure 6a, there is an increase and then a decrease in absorption that is seen in both the in situ and remotely-sensed absorption values despite the remote sensing values being less than the in situ values. Any further attempts to develop methods to derive absorption from remote sensing should focus on generating a spectral slope that is accurate to the spectral slope in situ.

Future research on developing more accurate remote sensing algorithms for calculating absorption from CDOM in Maine estuaries should focus on calculating a spectral slope that is more in line with what is observed in situ. An algorithm developed for remote sensing in Maine estuaries should account for the optical complexity of estuaries and the assumptions made by those algorithms should reflect the properties of to a body of water whose absorption is heavily dominated by CDOM.

CONCLUSION

Chromophoric dissolved organic matter is important to ocean color remote sensing as it is used as a proxy for many things that do not have a visible marker like input of freshwater influence and DOC. Although this study does not have enough data to make any definitive statements on the effectiveness of current methods to derive absorption from remote sensing, it shows what next steps should be taken to develop methods to derive a_{CDOM} and eventually DOC from remote sensing products. There should be a focus on ensuring that the spectral slope calculated from new remote sensing methods are accurate to the spectral slope measured in situ as even minor differences can increase exponentially in shorter wavelengths.

LIST OF REFERENCES

Alcântara, E., Bernardo, N., Watanabe, F., Rodrigues, T., Rotta, L., Carmo, A., Shimabukuro, M., Gonçalves, S., & Imai, N. (2016). Estimating the CDOM absorption coefficient in tropical inland waters using OLI/Landsat-8 images. *Remote Sensing Letters*, *7*(7), 661–670. https://doi.org/10.1080/2150704X.2016.1177242

Bailey, Sean (2024). *The official NASA/OB.DAAC Data Analysis Software*. NASA Ocean Color. https://seadas.gsfc.nasa.gov/

Balch, W., Huntington, T., Aiken, G., Drapeau, D., Bowler, B., Lubelczyk, L., & Butler, K. (2016). Toward a quantitative and empirical dissolved organic carbon budget for the Gulf of Maine, a semienclosed shelf sea. *Global Biogeochemical Cycles*, *30*(2), 268–292. https://doi.org/10.1002/2015GB005332

Cao, F., & Tzortziou, M. (2021). Capturing dissolved organic carbon dynamics with Landsat-8 and Sentinel-2 in tidally influenced wetland–estuarine systems. *Science of The Total Environment*, *777*, 145910. https://doi.org/10.1016/j.scitotenv.2021.145910

Cao, F., Tzortziou, M., Hu, C., Mannino, A., Fichot, C. G., Del Vecchio, R., Najjar, R. G., & Novak, M. (2018). Remote sensing retrievals of colored dissolved organic matter and dissolved organic carbon dynamics in North American estuaries and their margins. *Remote Sensing of Environment*, *205*, 151–165. https://doi.org/10.1016/j.rse.2017.11.014

Coble, P. G. (2007). Marine Optical Biogeochemistry: The Chemistry of Ocean Color. *Chem. Rev.*, *107*, 402–418. https://doi.org/10.1021/cr050350+

Haefner Jr. P. 1967. Hydrography of the Penobscot River (Maine) Estuary. Journal of the Fisheries Research Board of Canada. 24(7): 1553-1571. https://doi.org/10.1139/f67-128

Fichot, C. G., Tzortziou, M., & Mannino, A. (2023). Remote sensing of dissolved organic carbon (DOC) stocks, fluxes and transformations along the land-ocean aquatic continuum: advances, challenges, and opportunities. *Earth-Science Reviews*, *242*, 104446. https://doi.org/10.1016/j.earscirev.2023.104446

Lee, Z., Carder, K. L., & Arnone, R. A. (2002). Deriving inherent optical properties from water color: a multiband quasi-analytical algorithm for optically deep waters. *Applied Optics*, *41*(27), 5755.

Lee, Z., Weidemann, A., Kindle, J., Arnone, R., Carder, K. L., & Davis, C. (2007). Euphotic zone depth: Its derivation and implication to ocean-color remote sensing. *Journal of Geophysical Research: Oceans*, *112*(C3), 2006JC003802. https://doi.org/10.1029/2006JC003802

Loisel, H., Stramski, D., Dessailly, D., Jamet, C., Li, L., & Reynolds, R. A. (2018). An Inverse Model for Estimating the Optical Absorption and Backscattering Coefficients of Seawater From Remote-Sensing Reflectance Over a Broad Range of Oceanic and Coastal Marine Environments. *Journal of Geophysical Research: Oceans*, *123*(3), 2141–2171. https://doi.org/10.1002/2017JC013632

Mannino, A., Novak, M. G., Hooker, S. B., Hyde, K., & Aurin, D. (2014). Algorithm development and validation of CDOM properties for estuarine and continental shelf waters along the northeastern U.S. coast. *Remote Sensing of Environment*, *152*, 576–602. https://doi.org/10.1016/j.rse.2014.06.027

Mayer, L. M. (1982). Aggregation of colloidal iron during estuarine mixing: Kinetics, mechanism, and seasonality. *Geochimica et Cosmochimica Acta*, *46*(12), 2527–2535. https://doi.org/10.1016/0016-7037(82)90375-1

Michaud, C. (2024). *Using CDOM optical properties to estimate its source, distribution, and DOC concentration in Maine estuaries* [Undergraduate Honors Thesis, University of Maine]. University of Maine Honors Thesis Archive.

Pahlevan, N., Schott, J. R., Franz, B. A., Zibordi, G., Markham, B., Bailey, S., Schaaf, C. B., Ondrusek, M., Greb, S., & Strait, C. M. (2017). Landsat 8 remote sensing reflectance (Rrs) products: Evaluations, intercomparisons, and enhancements. *Remote Sensing of Environment*, *190*, 289–301. https://doi.org/10.1016/j.rse.2016.12.030

Penobscot. Maine Rivers. https://mainerivers.org/watershed-profiles/penobscot-watershed/

Rudoff, F., Ruffing, J., Ford, T. (1995). *Damariscotta River Estuary: a Management Plan*. https://digitalcommons.library.umaine.edu/cgi/viewcontent.cgi?article=1249&context=maine_env_organizations

Sheepscot River. Maine Rivers. https://mainerivers.org/watershed-profiles/sheepscot-river/

Snyder, J., Boss, E., Weatherbee, R., Thomas, A. C., Brady, D., & Newell, C. (2017). Oyster Aquaculture Site Selection Using Landsat 8-Derived Sea Surface Temperature, Turbidity, and Chlorophyll a. *Frontiers in Marine Science*, *4*, 190. https://doi.org/10.3389/fmars.2017.00190

Twardowski, M. S., Boss, E., Sullivan, J. M., & Donaghay, P. L. (2004). Modeling the spectral shape of absorption by chromophoric dissolved organic matter. *Marine Chemistry*, *89*(2004), 69–88. https://doi.org/10.1016/j.marchem.2004.02.008

USGS Earth Explorer [computer file]. USGS. https://earthexplorer.usgs.gov/ (Accessed September 2023)

Werdell, P. J., McKinna, L. I. W., Boss, E., Ackleson, S. G., Craig, S. E., Gregg, W. W., Lee, Z., Maritorena, S., Roesler, C. S., Rousseaux, C. S., Stramski, D., Sullivan, J. M., Twardowski, M. S., Tzortziou, M., & Zhang, X. (2018). An overview of approaches and challenges for retrieving marine inherent optical properties from ocean color remote sensing. *Progress in Oceanography*, *160*, 186–212. https://doi.org/10.1016/j.pocean.2018.01.001

AUTHOR'S BIOGRAPHY

Andrea Rudai is from Phoenix, MD. She first encountered marine science at a SEA GRANT summer camp in the third grade. After that, she knew that she was going to be a marine scientist. She hopes to be a good role model for her three younger siblings.